A DECIMAL COUNTER ELECTRON TUBE

By D. L. Hollway*

Summary

A scale-of-10 counter electron tube is described, in which incoming signals are counted by triggering a single electron beam through a closed sequence of 10 pairs of stable states. Each stable state results from potential drops maintained on deflecting electrodes by the distribution of the beam current.

Current distributions and deflecting electrode systems of fivefold symmetry, which together develop rotating deflexion fields suitable for counters, are considered and an expression is derived for the optimum proportions of the electrode system.

Other possible applications of the basic principle, the "self-rotating beam", to special purpose tubes are indicated.

I. INTRODUCTION

The need for counters operating at speeds higher than those possible with mechanical registers was realized first by nuclear physicists in recording signals from ionization chambers. An important advance was made when Wynn-Williams (1931) described a circuit of " a group of inter-connected thyratrons, which automatically switch one another into operation as the need arises, so that however rapidly particles are arriving, there is always a thyratron available for each particle ".

In later forms, electronic counters are now widely used in the measurement of frequency, time, and other quantities which may be converted to a frequency or count.

The chief requirement of any counter, whether mechanical or electronic, is a form of " memory " consisting of stable states, positions, or potential levels. It may be shown that at least $2N$ stable states are needed for a counter in the scale-of-N ; of these, N store the count in the intervals between incoming signals and the remainder hold the count during changeover. In mechanical counters such as cyclometers, clock escapements, and so on, it is simple to design the mechanism so that all of the $2N$ states are stable during any period of time. But the equivalent " completely stable " states in electronic counters require vacuum tubes or other comparatively costly " active " circuit elements. It is usual, therefore, to simplify these circuits by using " temporarily stable " states for storage during changeover. The crossed grid-to-plate condensers in the four double-triode scale-of-10 circuits are an example of this economy. Input shaping circuits ensure that the incoming signals are completed before the

* Division of Electrotechnology, C.S.I.R.O., University Grounds, Sydney.

stored charges decay. These counters represent such an efficient use of components that little further simplification seems possible in designs based on the use of conventional vacuum tubes.

In 1947, in collaboration with Mr. A. M. Thompson, the possibility of devising a single high-vacuum-tube decimal counter was considered by the author, and several forms were planned.* The objective of the subsequent development was a counter of small size, operating at low anode voltage, with a minimum of associated circuitry, which would maintain counting accuracy over a wide range of circuit conditions and to as high a frequency as possible.

II. Principle of Operation
(a) General Description

The counter is a high-vacuum tube in which counting is accomplished by successive displacements of a deflected electron beam through a number of stable positions (Hollway 1950). The operating principle may be explained by considering the simplified electrode arrangement shown in Figure 1.
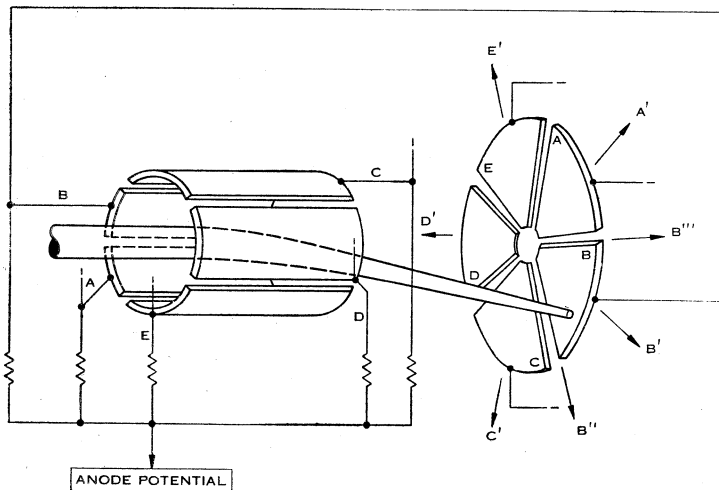

Fig. 1.—A simplified electrode system.

An electron beam enters, along the axis, a system of five similar deflector plates maintained near the potential of the final anode by five equal series resistances. The beam forms a focused spot in the plane of the collecting segments, each one of which is directly connected to the correspondingly lettered deflector.

If one deflector, B, is lowered momentarily in potential, an electrostatic field is formed which deflects the beam away from deflector plate B and moves the spot in the direction of the arrow B'. The beam current which then flows to collector B will lower the potential of the collector, and hence of the deflector,

* It was found later that one of these early designs had been anticipated by a form of counter proposed by Snyder (1946).

sufficiently to maintain the deflexion. A similar stable condition is possible at each of the other collectors, after initial deflexion.

Now imagine the deflector plates to be turned about the axis one-tenth of one revolution clockwise, viewed in the direction of the beam. Deflexion of the spot in the new direction, B'', will cause part of the beam current to flow to collector C, which in turn moves the spot further across plate C. There are no stable regions and the spot rotates continuously in the clockwise direction. Similarly, if the deflectors are retarded in space phase with respect to the collectors, to B''', the motion is reversed.
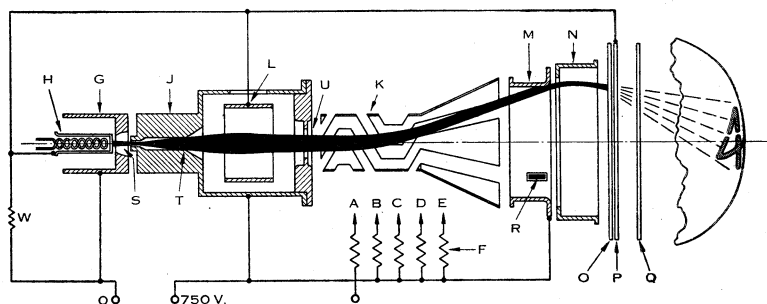

Fig. 2.—The electrode structure of the scale-of-10 counter, shown in section.
F, resistors connected to the collector plates A-E (shown in Figs. 4 and 5) ; G, grid ; H, cathode ; J, anode ; K, five deflectors ; L, focusing electrode ; M, positive ring ; N, trigger ring ; O, front collector plates ; P, suppressor ; Q, back collector plates ; R, carry-over electrode.

In the complete counter tube (Figs. 2 and 6) two separate sets of collector plates are used. The front group O is phased, with respect to the deflectors, for clockwise rotation and the back group Q is phased for reverse rotation. Openings are cut in the front group as shown in Figure 3. Thus, whenever the beam falls on the front plates it moves clockwise until part of the spot overlaps the radial edge of an opening and a fraction of the beam current flows to the back collectors shown in Figure 5. Further movement rapidly reduces the influence of the front system and increases that of the back, so that a state of angular equilibrium is reached, and the resultant deflexion is purely radial. Therefore the beam moves outwards until it is partially intercepted by the inside edge of a ring (M, Fig. 2), the " positive ring ", which is maintained at the potential of the final anode. Any further radial deflexion decreases the proportion of the beam which reaches the collectors, and the deflecting potentials are similarly reduced. Therefore a condition of equilibrium is reached when the beam is partly intercepted by the positive ring. Because the beam cross section is small in the plane of the ring, the radial deflexion remains almost unchanged by circuit variations or by the normal cycle of deflector potential changes which take place during the counting process.

In this way the angular position of the spot is always controlled by the deflector potentials and is sensitive to the collector currents, but these can have no effect on the radial position. The radial position is controlled only by the
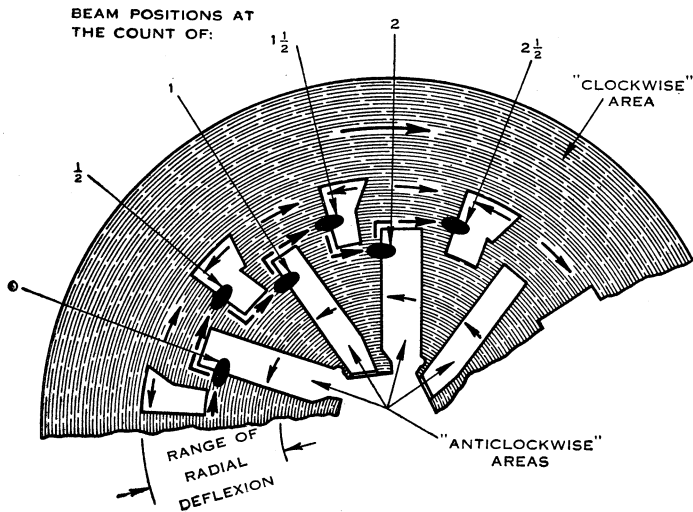
BEAM POSITIONS AT
THE COUNT OF:

Fig. 3.—A simplified view of the stable openings in the front collectors showing the counting sequence 0→1→2. Beam current falling on any part of the shaded area sets up potential changes which tend to move the spot clockwise. This clockwise area consists of the five separate electrodes shown in Figure 4.
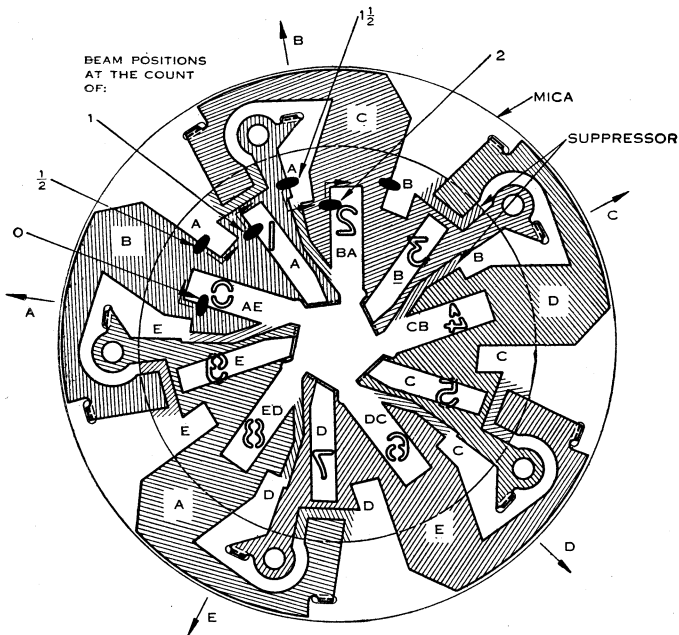
BEAM POSITIONS
AT THE COUNT
OF:

Fig. 4.—The collector assembly viewed in the direction of the beam, shown in relation to the directions of deflexion. When beam current reaches a shaded area, for example B at position 0, the corresponding deflector is lowered in potential producing a component deflexion in the direction of the arrow B.

trigger electrode (*N*, Fig. 2), a short cylinder which receives the signals to be counted.

When a positive going signal appears, the spot moves radially outwards from the position 0 (Figs. 3 and 4) until the outer edge of the slot is reached. Beyond this point the anticlockwise restraint from the back collectors is reduced and the spot moves clockwise to the outer opening $\frac{1}{2}$, which is stable for this and higher trigger potentials. The beam is held in position $\frac{1}{2}$ until the removal of the input signal moves the spot inwards, once more on to a clockwise region, causing a further rotation to position 1.
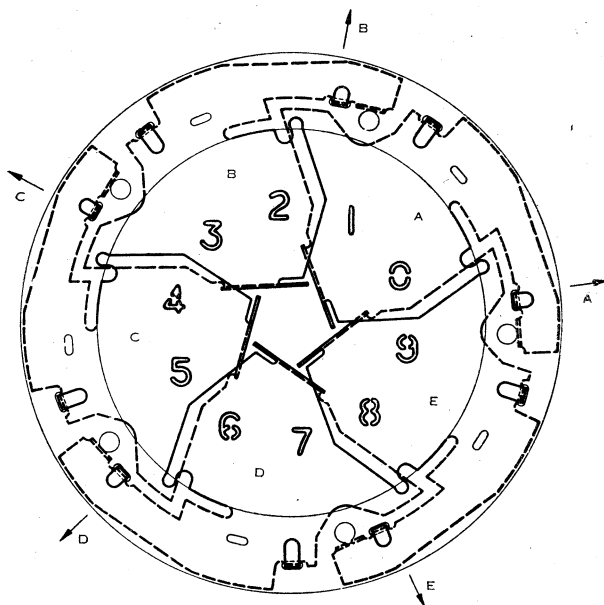

Fig. 5.—The back collector segments viewed from the screen against the direction of the electron beam.

Therefore each input signal moves the beam from one inner stable position to the next, increasing the stored count by one unit, and 10 waves cause the spot to complete a full revolution and return to the initial position. Because the states in which the beam is held during changeover are " completely stable ", the input signals may be of any duration and amplitude above the minimum values necessary to register a count.

Some interchange of secondary electrons is permitted between adjacent plates in both front and back groups in order to develop current waveforms corresponding to smoothly rotating deflexion fields, but complete suppression of secondaries between the two groups of collectors, and between the collectors and the other electrodes, is essential. This is ensured by keeping the trigger at a lower potential than the collectors, and by inserting a suppressor (*P*, Fig. 2) at cathode potential, between the front and back collectors. The suppressor has slots to match those in the front collectors. The outer 10 are larger than those in the collectors, so that the transmitted beam remains in good focus.

At the inner openings, however, the suppressor is formed so as to diverge the beam sufficiently to cover areas of the back collectors in which the figures 0–9 are cut, corresponding to the count positions. Electrons passing through the number openings continue to diverge, and project the number image,* enlarged eight times, centrally on the fluorescent end of the bulb.
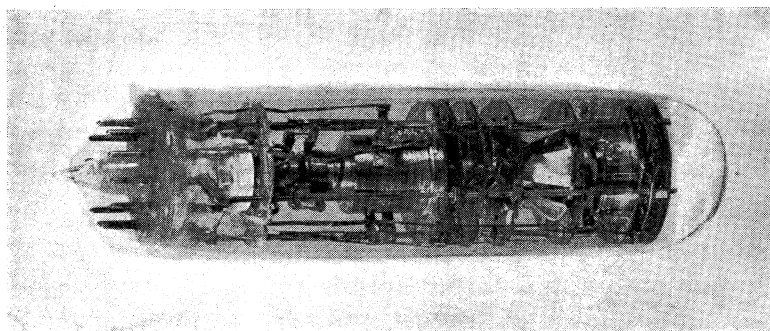

Fig. 6.—A scale-of-10 counter tube.

When the beam reaches the position $9\frac{1}{2}$, the " carry-over " electrode (R, Fig. 2) intercepts the current usually flowing to the positive ring. This produces a negative pulse at R which is coupled to the trigger of the next counter as described in Section IV.

The principles underlying the division of the beam current between the collectors at each of the stable states will now be considered.

(b) The Deflector Potential Waveforms

In describing the operation of the counter it has been stated that the beam current falling at any point on the front group of collectors sets up a deflexion field which tends to move the spot further in the clockwise direction, that is, at any spot position, the current to the front group corresponds to a radial deflexion component at an angle, α, in advance of the actual position of the spot.

The values of α and the corresponding angle of the backward component depend upon the design of the collector plates and other electrode dimensions including the angular relationship between the collectors and the deflectors. Thus, variations within the electrode constructional tolerances cause variations in α, which the design value must be large enough to absorb in addition to the margin needed for protection against circuit and external disturbances. The tube will count incorrectly if either angle is reduced to zero in any region of the collector circumference.

As perturbations may occur with equal probability in the backward or forward directions and at any spot angle, it is assumed, as a design basis, that

* This method of number projection is preferable to an earlier form using electrostatic projection lenses, because it results in a simpler collector system and only the small fraction of the beam passing through the numbers is lost from the back plates ; also the images are always in sharp focus and satisfactory projection is maintained for a wider range of trigger potentials.

both components should be equal, equally spaced at $+$ and $-\alpha$ with respect to the direction of the spot, and that α should remain constant. By this concept the components follow the spot in its movement around the circumference, and thus the stability of all states is essentially the same.

In early experiments it was found that, in positions almost midway between the deflexion directions of two deflector plates, the angular position of the spot was sufficiently sensitive to differential changes in the potentials of only those two deflectors, to provide highly stable states. For this condition $\alpha \approx \pm 36°$. Too small a value of α means reduced stability, but if α is made unnecessarily large beam current is " wasted ", as a larger current is needed for a given radial deflexion.
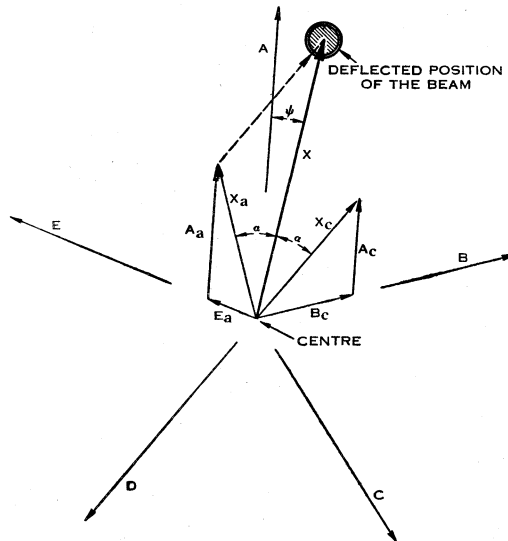

Fig. 7.—Components of the beam deflexion.

The individual collector currents needed to generate rotating fields of this kind are found from the vector diagram shown in Figure 7. The directions A to E are those of the five deflector plates ; that is, the spot would be moved in the direction A by making the potential of deflector A less positive   The angle of the spot deflexion vector $\bar{X}$, is ψ, measured to A as a reference. The clockwise and anticlockwise components of $\bar{X}$, $\bar{X}_c$ and $\bar{X}_a$, therefore fall at angles $\psi + \alpha$ and $\psi - \alpha$, and it is assumed that each component is formed of contributions from the two deflectors nearest in direction to its angular position. For example, in Figure 7, $\bar{X}_c$ falls between A and B so that $\bar{X}_c = \bar{A}_c + \bar{B}_c$.

Thus

$$\bar{X} = \bar{X}_c + \bar{X}_a,$$

$$|X_c| = |X_a| = |X|/2 \cos \alpha, \quad \dots\dots\dots\dots (1)$$

and the contribution of deflector A is

$$|A_c| = \frac{|X|}{2 \cos \alpha \sin (2\pi/5)} \sin \left(\frac{2\pi}{5} - |\psi + \alpha|\right). \quad \dots\dots (2)$$

As the collector currents may become zero, but may not change in sign, negative values of the sine term in (2) are replaced by zero.

When the clockwise component $\overline{X}_c$ is resolved in this way, for $\alpha=27°$, the required current waveforms at the front group of collectors appear as shown
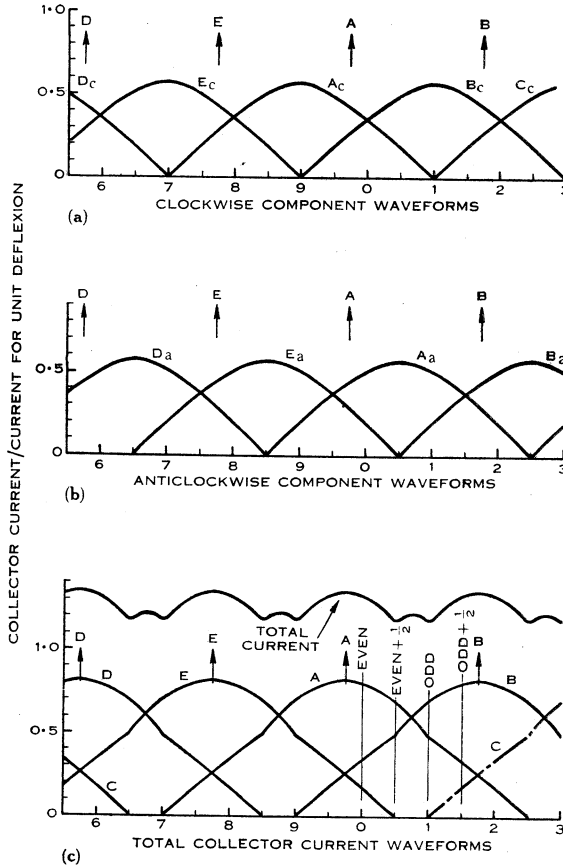

Fig. 8.—Calculated waveform of the rotating field components shown in Figure 7 for $\alpha=27°$.

    (a) The clockwise component.

    (b) The anticlockwise component.

    (c) The total deflexion.

in Figure 8 (a). The waveforms of the anticlockwise component (Fig. 8 (b)) are found in a similar way. The total deflexion by A is therefore $\overline{A}=\overline{A}_c+\overline{A}_a$ and

$$| A |=\frac{| X |}{2 \cos \alpha \sin (2\pi/5)}\left[\sin\left(\frac{2\pi}{5}-| \psi+\alpha |\right)+\sin\left(\frac{2\pi}{5}-| \psi-\alpha |\right)\right]. \quad .. \quad (3)$$

The waveforms calculated from (3) for $\alpha=27°$, shown in Figure 8 (c), are used as a basis for the counter design, although some compromise must be made to simplify the collector shapes.

The stable positions are spaced at approximately 18° intervals symmetrically about the directions of the deflector plates as shown in Figure 8.   In 10 of the positions it is essential to divide the beam current between three collectors, as in position 0 (Fig. 8 (c)), and this is done by allowing some secondary electrons to pass from the back collector plate A to E.   The secondary current is controlled by the field provided in the design of the collector assembly, and in similar tubes the distribution is quite repeatable.   The collector shape seen above each of the odd states in Figure 4 is used also to transfer current to the following plate.
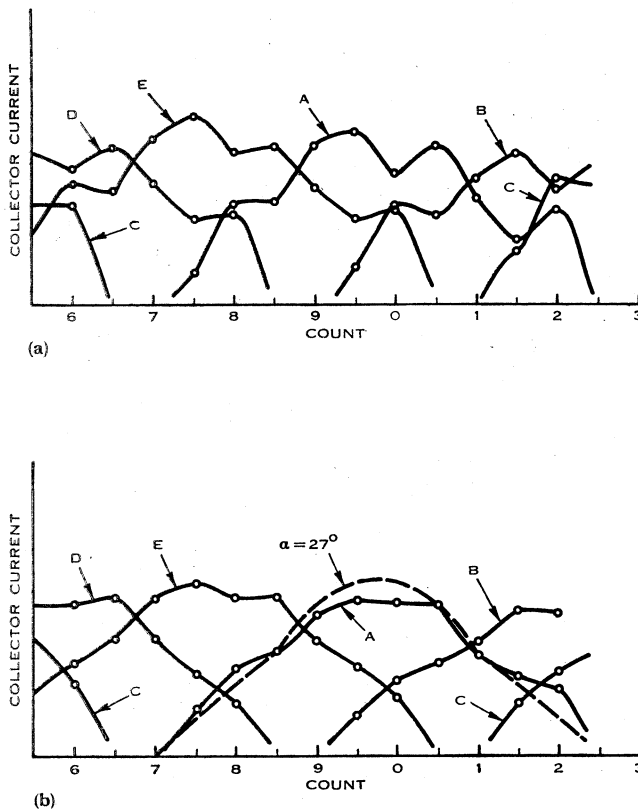

Fig. 9.—Waveform of the collector currents measured on experimental counters.

    (a) An unstable form.

    (b) A stable form.

The two examples of measured collector current waveforms drawn in Figure 9 (a) and (b) show the effect of a change in the division of the back collector current at the even states.   In (a), for example at position 0, the current to E is too great in comparison with A, and the stability is improved when this is corrected as shown in (b).

The deflector designs considered in the following section are chiefly those suited to the waveforms given by equation (3), $\alpha=27°$, and in Figure 8 (c).

III. The Electrode Structure
(a) *The Deflexion Field*

If an initially well-focused electron beam is deflected by reducing the potential of one or two of the five plates of the simple deflector system shown in Figure 1, the circular spot is broadened into an arc. The distorted spot is narrow in the radial direction, but the more important circumferential dimension, which must not exceed an 18° arc, cannot be reduced to the original size by the adjustment of the potential of the focusing electrode. A deflexion field causing this distortion may be termed " divergent ". The opposite form of distortion is shown when the beam is deflected by lowering four plates of the same system equally in potential, or by raising one ; the spot then appears as a radial line, which it is comparatively easy to compress into a spot after deflexion. Therefore it is desirable that the deflexion fields should be either convergent or distortion-less, rather than divergent. For this reason the simple system of five straight plates is not suited to the waveforms of Figure 8 in which groups of two or three plates contribute to the field.

A more uniform field is created by plates extending around an arc greater than $2\pi/5$, and since each plate may occupy only one-fifth of the total surface area of the deflecting cylinder, the effect of larger angles is obtained by twisting the plates into a helical or spiral form.*

It was first confirmed experimentally that a degree of spiralling is effective in reducing the distortion. The changes are most readily shown, however, by the method described in Appendix II, in which the spiralled plates are replaced by an equivalent cylinder varying in potential around the circumference, but constant in the axial direction. The fields are then calculated or measured from models in an electrolytic tank. The values of deflexion field shown in Figures 10 and 11 were determined in this way, and show the effect of increasing the twist of the deflecting plates from zero to one full turn around the deflecting cylinder. The twist of the plates is given as a fraction of one turn by the first figure of the designation, for example 0·6 in 0·6–2. Because the shape of the deflecting field varies cyclically with the angle of deflexion of the spot, ψ, two curves are drawn for each value of twist. These correspond to the two extremes of the variation, one of which occurs when the spot is in line with the direction of a deflector plate, and the second when it is midway between the directions of two adjacent plates. The plate potentials are shown also in Figure 10 ; these are based upon the waveforms of Figure 8 (c).

The curves of field gradient in the central plane (Fig. 10) show that, as the twist of the spiral is increased from zero in the topmost curves, the field becomes more uniform, although lower in intensity, until the spiral extends half way around the circumference, as in the curves 0·5–2, 0·5–3. At larger angles the

---

* A second method of reducing the distortion has also been used, in which 10 or a higher multiple of five straight plates are spaced equally around the deflecting cylinder and connected together to form five similar groups. The central field of a system of 10 plates connected 1–4, 3–6, 5–8, 7–10, 9–2 is convergent, but the deflector diameter must be at least three times larger than the beam, when used with the waveforms of Figure 8 (c).
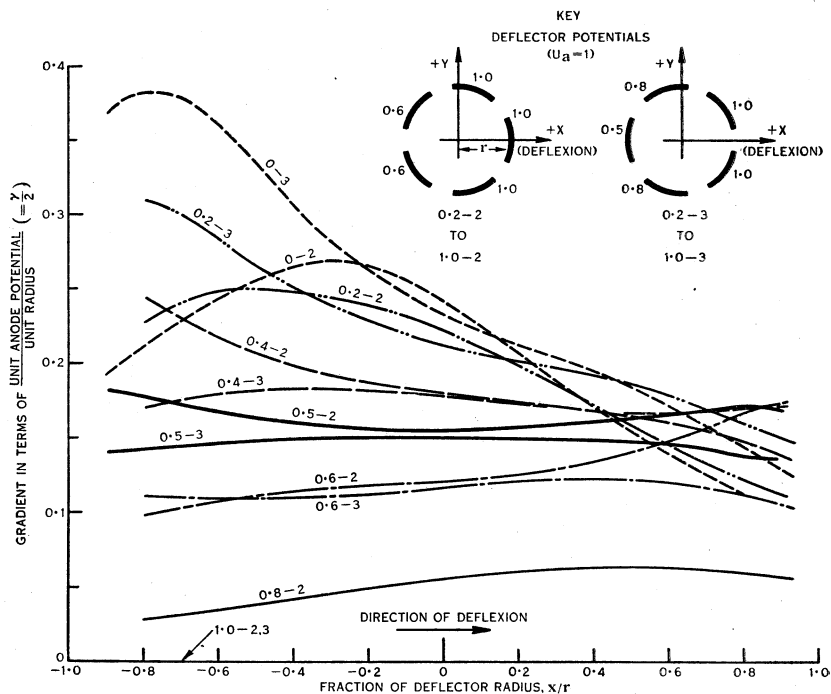
Fig. 10.—The deflexion fields of spiral deflectors.
The most uniform fields are those of curves 0·5–2, and 0·5–3. In this designa-
tion 0·5 indicates that the spiral electrode makes one-half of one complete
rotation about the deflecting cylinder, and 2, 3, refer to the number of deflectors
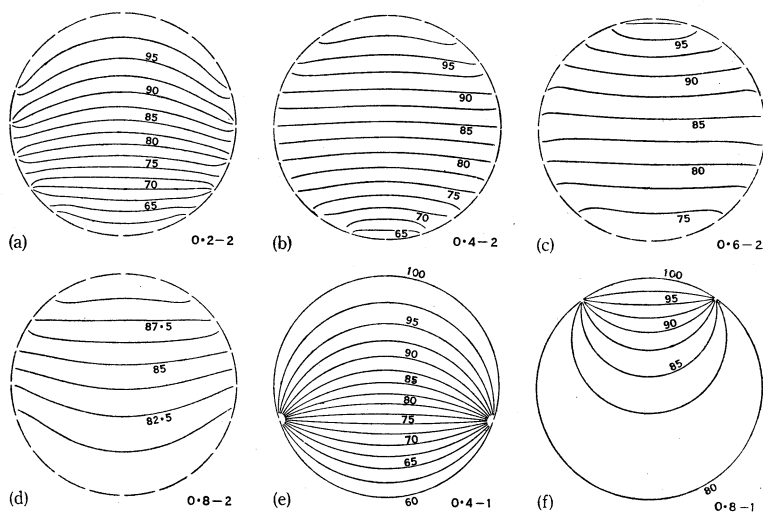lowered in potential together as shown in the key.

Fig. 11.—Equipotential patterns of the deflexion fields.
The direction of deflexion is upwards in each field, and the designations
correspond with those of Figure 10.

deflexion sensitivity falls more rapidly but the central field becomes slightly convergent, indicated by the upwards slope of the gradient curves in the positive direction, the direction of beam deflexion.

The same changes are shown over the whole area of the potential patterns in Figures 11 (a)-(d). The field becomes more uniform as the twist increases from $0 \cdot 2$ to $0 \cdot 6$, and finally convergent at $0 \cdot 8$, shown by the curvature (concave upwards) of the equipotentials. In this sequence the fall in deflexion sensitivity is indicated by an increase in the spacing of the contours. Although these equipotentials apply to a spot position midway between the directions of two deflectors, similar changes appear also in the group measured for a position directly in line with a deflector when the spot is controlled by three adjacent plates.

These patterns may be compared with the fields of single plates occupying $0 \cdot 4$ and $0 \cdot 8$ of one rotation, shown in Figure 11 (e) and (f). The strong convergence of the single $0 \cdot 8$ spiral, which could be used to maintain a sharply focused spot at a higher beam current, is always lost when two or three plates contribute to the field. Spiral deflectors, twisted in the range $0 \cdot 3$–$0 \cdot 5$ of one rotation and including the straight sections shown in Figure 1, have been used in recent counters as a compromise between deflexion sensitivity and distortion.

(b) The Electrode Proportions and the Highest Counting Frequency

The problem of selecting the major dimensions of the electrode system to attain the highest counting frequency will now be considered. As in other electron beam tubes the performance depends upon a large number of variables including the beam current, the anode potential, the change in deflector potential during counting, the spot radius, and all the main electrode dimensions. Several of these are made interdependent by the operating principle and some limits are set by difficulties in construction, but the dominating requirement is the need to maintain maximum stability in all states.

It may be assumed that if the operating principle remains unchanged, the highest counting frequency of a scale-of-N tube is proportional to

$$\frac{I}{C(U_a - U_d)/N}, \quad \cdots\cdots\cdots\cdots\cdots\cdots \text{(4)}$$

where $C =$ an effective value of capacitance associated with one of the deflector-collector combinations,

$I =$ beam current,

$U_a - U_d =$ the difference between the highest and lowest potentials reached by a deflector during counting. $(U_a - U_d)/N$ is a measure of the deflector potential change taking place between one state and the next.

At this point it is convenient to divide the problem into two parts, and to consider firstly the best size of the tube as a whole, and secondly the best proportions or shape of the electrode system.

The first question is answered by the scaling relation termed by Moss (1945) " The Principle of Geometrical Similitude ". This principle states that if all the dimensions of an electrode system are multiplied by some constant factor, the

operating potentials and beam current remain unchanged. However, the capacitance C will vary linearly in proportion to the scale factor, and therefore the counter as a whole should be reduced in size as far as the methods of construction allow.

In the second part of the problem it will be assumed that the overall size is chosen so that the capacitance C remains constant. Apart from its simplicity, this assumption of constant capacitance is more in accordance with a limitation set by the difficulty of constructing very small components than the alternative of keeping any one dimension constant. Thus the electrodes must be proportioned to make the term $NI/(U_a-U_d)$ a maximum, and for convenience in analysis, the dimensions will be found in terms of the initial radius of the electron beam cross section.

The allowable spot radius s depends upon the radial deflexion of the beam at the collectors. For stability, s may not exceed the value derived in Appendix I, and given by

$$l = s^{0 \cdot 65} d^{0 \cdot 35} U_a{}^{0 \cdot 5} 2(4N/\pi)^{0 \cdot 65}/\gamma^{0 \cdot 5}(U_a-U_d)^{0 \cdot 5}. \quad \ldots \ldots \text{ (5)}$$

It has been shown (Hollway 1952) that the greatest value of beam current I, in milliamperes, which can be concentrated into a spot of radius s, is governed by the length of the beam and the potential (in volts) where

$$l = 0 \cdot 39 s^{0 \cdot 4} U_a{}^{0 \cdot 75}/I^{0 \cdot 5}. \quad \ldots \ldots \ldots \ldots \text{ (6)}$$

Therefore, on combining equations (5) and (6),

$$\frac{NI}{(U_a-U_d)} = 0 \cdot 028 U_a{}^{0 \cdot 5}\gamma/d^{0 \cdot 7} s^{0 \cdot 5} N^{0 \cdot 3}. \quad \ldots \ldots \ldots \text{ (7)}$$

Thus, when the capacitance C is constant, the frequency varies as $s^{-0 \cdot 5}$, so that the spot radius should be kept small. This is explained by the fact that, if the length of the structure is increased, the allowable spot radius increases (with the deflexion distance) in proportion to $l^{1 \cdot 54}$; but the actual spot radius, controlled by space-charge defocusing, rises more rapidly, as $l^{2 \cdot 5}$, so that a small value of l, and of s, is needed.

The possibility of raising the sensitivity (γ) and improving the uniformity of the deflexion field, which sets a lower limit to d, has been discussed in Section III (a).

When equation (5) is compared with results measured on experimental counters, close agreement is found. However, the beam current predicted by equation (6), assuming beam potentials of U_a and U_d, is 4 and $1 \cdot 5$ times the observed maximum because spherical aberration in the objective lens, deflexion defocusing, and the geometrical spot size cannot be made negligible.

IV. PERFORMANCE

The electrical operating characteristics of the counter are contained in Figures 12 and 13. The anode characteristic (Fig. 12) is based upon the current flowing to the positive ring. During counting the beam current must be sufficient to hold the beam against the edge of the positive ring so that it is partially intercepted. At the $9\frac{1}{2}$ state, the ring current is transferred to the carry electrode

(R, Fig. 2) where it may be measured as an indication of the correct grid bias at any anode potential. Figure 12 shows the change in carry current with anode voltage, at different values of cathode resistance. The upper limit to the carry current is set by the increase in spot size which takes place when the beam current is raised. In the operating range the anode potential is not critical and no stabilization is necessary.
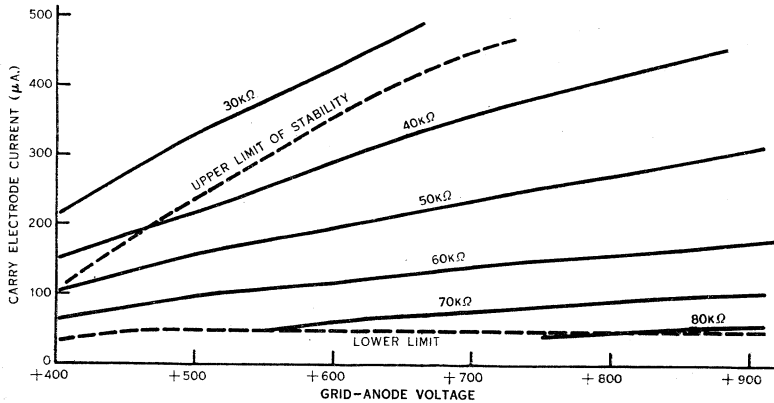

Fig. 12.—Anode potential characteristic.
The curves show stable operating ranges for different values of cathode
(self-bias) resistance.

The potential levels at which changes occur between states and the ranges of stability are shown in the trigger characteristic of Figure 13. The extent of the range in the negative direction may be explained by the rapid decrease in the trigger sensitivity as the beam moves inwards. In the positive direction
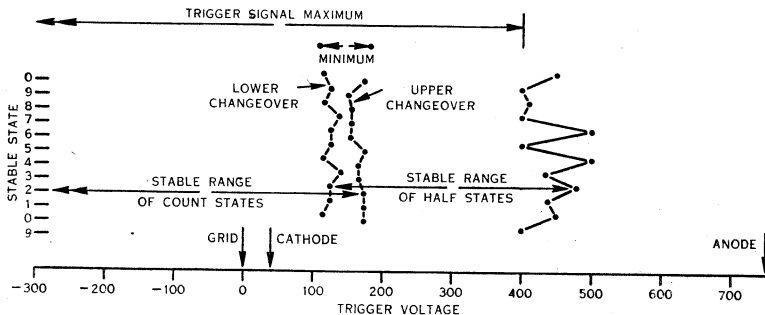

Fig. 13.—Trigger characteristic.
The measured points define ranges of the trigger potential in which the count
and intermediate positions of the beam are stable.

the range ends when the trigger fails to suppress secondary electrons from the front plates. The power supply and coupling circuits may be designed from these characteristics.

The complete circuit of a counter having four scale-of-10 stages is shown in Figure 14. Four of the five collector resistances in each stage are returned to the anode line, which is held at approximately 750 V. ; the resistances connected

to the 0–1 plates are returned to the same potential through the reset push button.

When a negative-going signal appears at the input terminals, the grid of the first triode section falls, raising the trigger of the first counter and bringing the beam into an intermediate position. The supply potential of the triode anode resistors is chosen within the stable range of the intermediate states, so that the incoming signals are not restricted in amplitude. The count is completed when the trigger potential falls to the lower change-over point. The usual pulse forming or " trigger circuit ", needed with multiple tube counters operating from zero frequency upwards, is unnecessary because discontinuities result from the form of the collector plates. Also, because the speed at which the beam
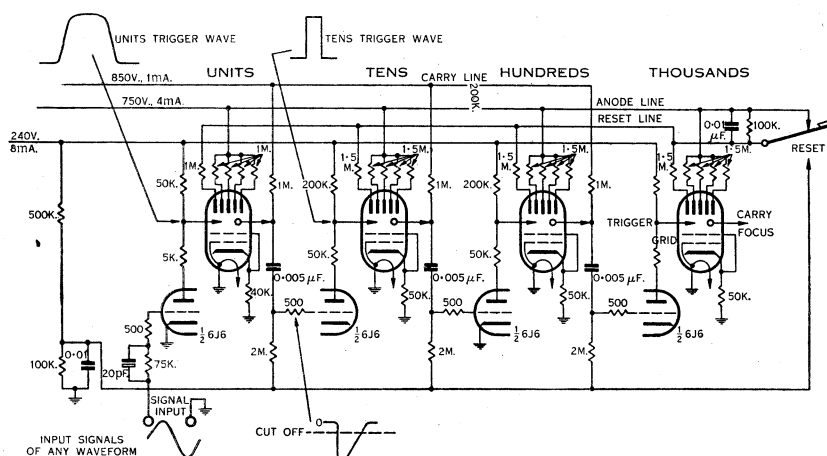

Fig. 14.—Circuit of a complete four-tube counter.

rotates is independent of the rate of change of the trigger potential, the pulse generated at the carry electrode when the beam falls into the $9\frac{1}{2}$ position is always sharp and may be coupled by means of a capacitance to the grid of the second triode, without thereby setting a lower limit to the speed of counting.

Between pulses the triode sections draw grid currents of 20–50μA. through their grid resistances. This eliminates stray signals below a certain amplitude, for example those appearing at the carry electrode before the $9\frac{1}{2}$ state is reached.

In resetting the counter, the line connected to the resistors of the 0–1 collectors is lowered momentarily in potential, bringing all the electron beams to the zero positions. Carry-over pulses are often produced during resetting and these are suppressed by increasing the grid currents of the triodes through the additional circuit from the reset push button shown in Figure 14.

At frequencies approaching the highest speed of counting, there is a fall in the amplitude of the carry signals caused by failure of the deflectors to return to the full anode potential in the intervals between transits of the beam. Beyond the upper limit the beam fails to complete one rotation during 10 incoming signals and the divisor rises to values higher than 10. This limit has been measured at frequencies between 70 and 180 kc/s., depending upon the circuit conditions.

V. FUTURE DEVELOPMENTS

The basic principle of the " self-rotating " beam may be applied to a number of tubes for special purposes. One of these is a reversible counter which will add or subtract signals from the stored count. For subtraction, a third ring of intermediate stable states can be used, on a smaller radius than the count positions ; change-over on the inner path is in the anticlockwise direction, so that each negative trigger signal subtracts one unit from the count.

Either the reversible form or the normal counter tube may be constructed with two or more trigger rings instead of one ; this would allow signals from two or more sources to add to or subtract from the count, while maintaining electrical isolation between the inputs. If one trigger receives only positive signals and the second is restricted to negative ones, coincident signals will cancel and produce no change in the count.

By a modification to the collector system, the counter may be extended to accept without error coincident positive signals from a pair of triggers, combinations of positive and negative, and coincident negative signals. This is accomplished by the use of an additional ring of 10 stable states, in a scale-of-10 tube, on a larger radius than the half states ($1\frac{1}{2}$, $2\frac{1}{2}$, $3\frac{1}{2}$, etc.). States in the outer ring lie midway between the half states, and are therefore in the same angular positions as the count states (1, 2, 3, etc.). The outer states may be identified as 1′, 2′, 3′, etc. in correspondence with those in the inner ring. On this collector system the simultaneous arrival of two positive signals moves the spot, originally at the count of 3, for example, to $3\frac{1}{2}$ and beyond this to 4′ in the outermost ring. When the signals decrease, the spot moves on first to $4\frac{1}{2}$, and finally returns to 5, which is an increase in the stored count of two units. Thus to count accurately coincident signals from a number of input channels, the number of complete rings of states needed in addition to the " count " states is equal to the number of channels. The minimum value of the trigger signal rise time, which is not restricted in the simple counter, must be large enough in the coincidence form to allow the necessary angular rotation of the spot. Coincidence tubes, used in the product register of a decimal electronic computer, could accept carry-over signals occurring during arithmetic operations.

Scale-of-N counter tubes may be constructed on the same principle, either by changing the number of stable states in each collector or by changing the number of deflectors and collectors. For example a scale-of-12 may use six deflectors and collectors, each collector having four states, as in the scale-of-10. For a scale-of-5, five deflectors and collectors having two stable states in each collector would be more suitable.

To provide separate output signals corresponding to each digit, for some applications it may be necessary to construct a scale-of-10 counter with 10 plates instead of five, and it would be simpler to use untwisted deflectors raised in potential by secondary emission. This would allow the use of strongly convergent fields (see Section III (a)), either for the deflexion of a beam, or to create localized gradients at a cathode surface to direct and focus the electron stream without the need for an electron gun or deflector system.

H

VI. Acknowledgments

The author wishes to record appreciation of the interest and encouragement of Professor D. M. Myers, of the Electrical Engineering Department, University of Sydney, the contribution of Mr. A. M. Thompson, noted earlier, and the cooperation of the staff of the C.S.I.R.O. Valve Laboratory.

VII. References

Gabor, D. (1937).—*Nature* **139** : 373.
Hollway, D. L. (1950).—*Nature* **165** : 856.
Hollway, D. L. (1952).—*Aust. J. Sci. Res.* A **5** : 430.
Moss, H. (1945).—*J. Brit. Instn. Radio Engrs.* **5** : 204.
Salinger, H. (1937).—*Electronics* **10** : 50.
Snyder, R. L. (1946).—U.S. Pat. 2,404,106.
Wynn-Williams, C. E. (1931).—*Proc. Roy. Soc.* A **132** : 295.

Appendix I

The Allowable Size of the Deflected Spot

In a scale-of-N counter each one of the $2N$ stable states consists of two regions, as described in Section II (*a*). It will be assumed that the electron spot, of radius s, must fall completely within one of these regions in order to develop fully the stable margins at each state. Thus the necessary deflexion x is given by

$$x = 4Ns/\pi. \quad \dots\dots\dots\dots\dots\dots\dots \quad (8)$$

An expression for the deflexion will now be derived from the electrode geometry.

To improve the deflexion sensitivity practical deflectors are bellmouthed (e.g. Fig. 2) and it is desirable to include this shaping in the derivation. It is assumed therefore that the inside radius of the deflector surface follows the central trajectory of the deflected beam but at a distance d from it. As in Section III (*b*), the initial radius of the electron beam is taken as the unit of length, and the quantities d, l, x, and s, represent numbers of beam radii.

The motion of an electron entering the deflector along the central axis is given by

$$d^2x/dt^2 = e\gamma(U_a - U_d)/m(x+d) \text{ (e.s.u.)}, \quad \dots\dots\dots \quad (9)$$

where γ is constant for a particular deflector design and waveform, relating the intensity of the deflexion field to $(U_a - U_d)/(x+d)$. (Values of γ for a number of different deflectors are shown in Figure 10.)

Multiplying both sides of equation (9) by dx/dt, integrating and inserting the initial conditions $x=0$, $dx/dt=0$, when $t=0$:

$$\frac{dx}{dt} = \sqrt{\frac{2e}{m}\gamma(U_a - U_d)\ln\left(\frac{x}{d}+1\right)} \text{ (e.s.u.).} \quad \dots\dots\dots \quad (10)$$

Since the length l is measured along the beam (from $l=0$, $x=0$) and the beam potential is near U_a throughout the trajectory, as shown in Figure 11, $\sqrt{2e/mU_a}$ (e.s.u.) may be substituted for dl/dt, giving

$$\frac{dx}{dl} = \sqrt{\gamma(1 - U_d/U_a)\ln\left(\frac{x}{d}+1\right)}. \quad \dots\dots\dots\dots \quad (11)$$

On substituting $\ln(x/d+1)=g^2$,

$$l=\frac{2d}{\sqrt{\gamma(1-U_d/U_a)}}\int_0^{\sqrt{\ln(x/d+1)}}e^{g^2}dg. \quad \dots\dots\dots \quad (12)$$

This form of integral appears in analyses of space charge defocused beams, and cannot be solved in terms of usual functions. However, in the present application, (12) is used to find the final deflexion x of the beam after travelling a distance l, so that values of x/d outside the range $1 < x/d < 10$ are not needed in practice. With this restriction, a simple substitution is possible and

$$l \approx 2d(x/d)^{0.65}/\gamma^{0.5}(1-U_a/U_d)^{0.5}. \quad \dots\dots\dots\dots \quad (13)$$

Therefore combining equations (8) and (13), the greatest allowable spot radius s is given by the relation

$$l \approx s^{0.65}d^{0.35}U_a^{0.5}2(4N/\pi)^{0.65}/\gamma^{0.5}(U_a-U_d)^{0.5}. \quad \dots\dots \quad (5)$$

APPENDIX II
The Determination of the Deflexion Fields and Electron Paths

The circle $AHCD$, of radius r (Fig. 15) represents a cross section through a long deflector system of which the dotted segment DAH is at zero potential and the remainder of the circumference is at the potential U_0. To convert the electric field pattern of the deflector to a simple form, the section is transformed conformally by inversion with the point H as centre, so that any point M having coordinates x, y in the original section is represented by M' in accordance with the transforming equation,

$$HM \cdot HM' = (2r)^2. \quad \dots\dots\dots\dots \quad (14)$$

The dotted segment DAH becomes the straight line $D'A'H'$ at zero potential, and $D'C'H'$ represents the remainder of the circumference at potential U_0; the X-axis is converted to the semicircle $A'C'$ having D' as centre.

In the half-plane P, lying to the right of $H'D'H'$, which corresponds to the interior of the circle, the equipotentials are all straight lines radiating from D', so that the potential U_{xy} of point M is the potential of M', or

$$U_{xy}=U_0\beta/\pi.$$

From the geometry of the figure, β may be found in terms of x, y, and θ, giving

$$U_{xy}=\frac{U_0}{\pi}\left[\theta+\cot^{-1}\tfrac{1}{2}\left\{\frac{\sin\theta}{x/r+\cos\theta}\left(1-\frac{(y/r)^2}{\sin^2\theta}\right)-\frac{x/r+\cos\theta}{\sin\theta}\right\}\right]. \quad \dots\dots \quad (15)$$

The potential along the X-axis may be found by setting $y=0$ in (15), or directly from the figure, since $HD'=D'G'=D'E'$, $\angle G'D'E'=2\varphi$, and therefore

$$U_x=U_0(\theta+2\varphi)/\pi=\frac{U_0}{\pi}\left[\theta+2\tan^{-1}\left\{\frac{x/r+\cos\theta}{\sin\theta}\right\}\right]. \quad \dots\dots \quad (16)$$

Because the equipotentials in the P-plane are straight lines through D', they form circles in the XY-plane passing through H and D. The radius of an equipotential U_x which crosses the X-axis at x, is therefore

$$R_x = r\left(\frac{x/r + \cos\theta}{2} + \frac{\sin^2\theta}{x/r + \cos\theta}\right)$$

and, by substitution from (**16**),

$$R_x = r\sin\theta/4\sin\left(\frac{\pi U_x}{U} - \theta\right). \quad \ldots\ldots\ldots\ldots (17)$$
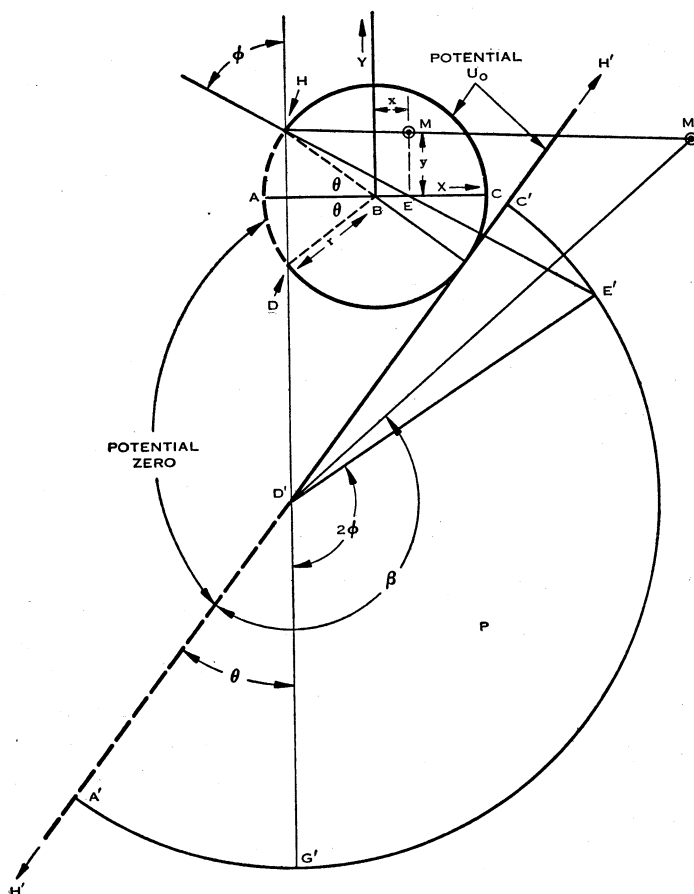

Fig. 15

The gradient along the X-axis is given by the differentiation of (**16**),

$$\frac{\partial U_x}{\partial x} = \frac{U}{\pi r}\frac{2\sin\theta}{(x^2/r^2 + 2x/r\cos\theta + 1)}. \quad \ldots\ldots\ldots (18)$$

The maximum value of the gradient occurs at $x/r = -\cos\theta$, that is, on the chord joining the ends of the segment, which is also an equipotential of infinite radius. Thus as θ is increased to approach $\pi/2$, the position of the maximum

moves from negative values of x/r towards the centre of the deflexion field where it coincides broadly with the position of the electron beam cross section. This more favourable position of the maximum explains the comparatively small decrease in the central gradient shown by the sequence of the topmost six curves in Figure 10 and the subsequent rapid drop in sensitivity when the twist is increased beyond $\theta/\pi = 0 \cdot 5$.

Equation (18) has been used to find the deflexion field intensity of spiralled deflectors by the following approximate analysis. First the potentials of the five plates, corresponding to a chosen position of the spot, are found as described in Section II (b). The spiralled deflector system is then converted to one similar in general form but composed of untwisted strips. Each strip (of angular width θ_1) is given a potential U'_θ equal to the mean potential of the corresponding surface area of the spiralled system. Thus, for a cylindrical array of length Z_d,

$$U'_\theta = \frac{1}{\theta_1 Z_d} \int_0^{Z_d} \int_{\theta - \theta_1/2}^{\theta + \theta_1/2} U \, \mathrm{d}\theta \mathrm{d}z. \quad \ldots\ldots\ldots\ldots (19)$$

It is convenient to set $\theta_1 = 18°$ and to integrate graphically. The gradient is then calculated from these values of U'_θ by superposition in equation (18). However, it is usually quicker to set up the potentials U'_θ in an electrolytic tank model of the untwisted system, and to measure the gradient and potential directly. The accuracy of the tank measurements, judged from a comparison between measured and calculated curves of Figure 10, was approximately ± 3 per cent. of $\partial U/\partial x$.

To find the electron paths in these deflexion fields, which are non-uniform but symmetrical about the X-axis, the " circle method " (Salinger 1937) has been used in both the XY- and XZ-planes. Recently an electron tracer based on Gabor's Tangent Bridge (Gabor 1937) was constructed and found to be quicker and more accurate. However, in problems of figure projection, the distribution of beam current between the collectors, constructional tolerances and others, it is necessary to supplement electron path tracings with measurements made on trial electrode assemblies.